Muon g–2 in two-Higgs-doublet models

Eung Jin Chun*
Korea Institute for Advanced Study, Seoul 130-722, Korea

Updating various theoretical and experimental constraints on the four different types of two-Higgs-doublet models (2HDMs), we find that only the "lepton-specific" (or "type X") 2HDM can explain the present muon g−2 anomaly in the parameter region of large $\tan\beta$, a light CP-odd boson, and heavier CP-even and charged bosons which are almost degenerate. The severe constraints on the models come mainly from the consideration of vacuum stability and perturbativity, the electroweak precision data, the b-quark observables like $B_S \to \mu\mu$, the precision measurements of the lepton universality as well as the 125 GeV boson property observed at the LHC.

arXiv:1511.05225v1 [hep-ph] 16 Nov 2015

I. OUTLINE

Since the first measurement of the muon anomalous magnetic moment $a_\mu = (g-2)_\mu/2$ by the E821 experiment at BNL in 2001 [1], much progress has been made in both experimental and theoretical sides to reduce the uncertainties by a factor of two or so establishing a consistent 3σ discrepancy

$$\Delta a_\mu \equiv a_\mu^{\rm EXP} - a_\mu^{\rm SM} = +262\,(85)\times 10^{-11} \tag{1}$$

which is in a good agreement with the different group's determinations. Followed by the 2001 announcement, there have been quite a few studies in the context of 2HDMs [2–4], however, restricted mainly to the type I and II models out of four different types of 2HDMs ensuring natural flavour conservation. Considering the recent experimental development confirming more precisely the Standard Model (SM) predictions, including the discovery of the 125 GeV Brout-Egnlert-Higgs boson, it would be timely to revisit the issue of the muon g–2 in 2HDMs.

An additional contribution to th muon g–2 from an extra boson in 2HDMs, shown in Fig. 1, may be the origin of the positive excess in the Δa_μ. This can happen in the type II or X (lepton-specific) 2HDM which allows a light boson having large Yukawa couplings enhanced by $\tan\beta$. While the type II option is completely ruled out by now, the type X model [5] remains an unique option to explain the a_μ anomaly evading all the recent experimental constraints [6–9].

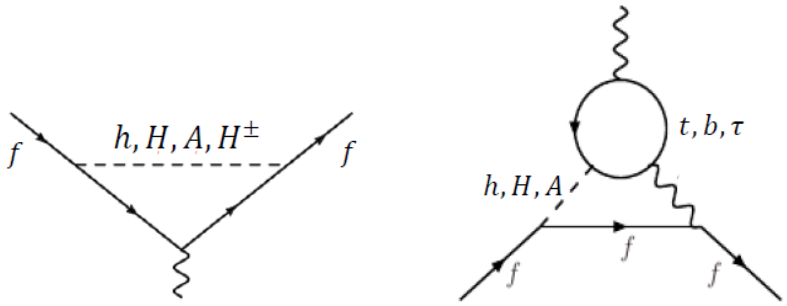

FIG. 1: One and two loop diagrams contributing to the muon g−2 in 2HDMs.

The previous studies on the muon g–2 in the type II 2HDM (2HDM-II) and various experimental constraints were nicely summarised in Ref. [3]:

*Electronic address: ejchun@kias.re.kr

- The one-loop correction mediated by a light CP-even (CP-odd and charged) boson gives a positive (negative) contribution to Δa_μ, and thus the current 3σ deviation can be explained by a CP-even boson lighter than about 5 GeV. However, such a light boson was already in contradiction to non-observation of radiative Υ decays $\Upsilon \to \gamma + X$.

- Contrary to the one-loop correction, the major two-loop contribution from the Barr-Zee diagram [10] mediated by a light CP odd (even) boson can give a sizable positive (negative) contribution to Δa_μ. Thus, a light CP odd boson A with large $\tan\beta$ can account for the muon g–2 deviation. However, most of the muon g–2 favoured region in the lower and upper M_A part are excluded by the LEP and TEVATRON search on $Z \to b\bar{b}A(b\bar{b})$, respectively, except a small gap of $M_A \approx 25 - 70$ GeV with $\tan\beta \gtrsim 20$.

- However, let us note that such a light A gives a huge contribution to $B_s \to \mu^+\mu^-$ as its rate is proportional to $\tan^4\beta/M_A^4$ [11], and thus the above gap is completely closed now by the LHC measurement which is consistent with the SM prediction [12].

Now the situation can be quite different in the type X 2HDM (2HDM-X) where all the extra boson couplings to quarks (leptons) are proportional to $\cot\beta$ ($\tan\beta$). Due to this, the 2HDM-X becomes hadrophobic in the large $\tan\beta$ limit invalidating most hadron-related constraints applied to the type II model. On the other hand, its leptophilic property brings sever constraints from the precision leptonic observables. The key features in confronting the type X model with the muon g–2 anomaly can be summarized as follows [6–9].

- As in the 2HDM-II, the one-loop correction with a light CP even boson H can account for the muon g–2 excess. While the Upsilon decay suppressed by $1/\tan^2\beta$ cannot provide a meaningful constraint, the Belle and LHCb searches for $B \to K\mu\mu$ shut down the muon g–2 favoured region except tiny gaps around $M_H \approx 3$ and 4 GeV [13]. In any case, such a light Higgs boson is excluded by the current measurement of $B_s \to \mu^+\mu^-$ even in the 2HDM-X where $\Gamma(B_s \to \mu^+\mu^-) \propto 1/M_H^4$.

- The Barr-Zee diagram with the tau lepton in the loop can account for the muon g–2 anomaly again in a parameter region of small M_A and large $\tan\beta$ evading all the constraints from the hardron colliders and the b-quark observables [6] except the process $B_s \to \mu^+\mu^-$ which rules out $M_A \lesssim 10$ GeV [7].

- However, the lepton universality test by HFAG [14] combined with the $Z \to \tau\tau$ decay turns out to limit severely the muon g–2 favoured region of the type X model [8] allowing (only at 2σ) a small region below $M_A \approx 80$ GeV and $\tan\beta \approx 60$ [9].

- With such a light A, the exotic decay of the 125 GeV boson $h \to AA$ or $AA^*(\tau\tau)$ becomes generically too large unless a certain cancelation is arranged to suppress the hAA coupling λ_{hAA} which turns out to be possible only in the wrong-sign limit of the lepton Yukawa coupling [7].

II. FOUR TYPES OF 2HDMS

Non-observation of flavour changing neutral currents restricts 2HDMs to four different classes which differ by how the Higgs doublets couple to fermions [16]. They are organized by a discrete symmetry Z_2 under which different Higgs doublets and fermions carry different parities. These models are labeled as type I, II, "lepton-specific" (or X) and "flipped" (or Y). Having two Higgs doublets $\Phi_{1,2}$, the most general Z_2 symmetric scalar potential takes the form:

$$\begin{aligned} V &= m_{11}^2|\Phi_1|^2 + m_{22}^2|\Phi_2|^2 - m_{12}^2(\Phi_1^\dagger\Phi_2 + \Phi_1\Phi_2^\dagger) \\ &\quad + \frac{\lambda_1}{2}|\Phi_1|^4 + \frac{\lambda_2}{2}|\Phi_2|^4 + \lambda_3|\Phi_1|^2|\Phi_2|^2 + \lambda_4|\Phi_1^\dagger\Phi_2|^2 + \frac{\lambda_5}{2}\left[(\Phi_1^\dagger\Phi_2)^2 + (\Phi_1\Phi_2^\dagger)^2\right], \end{aligned} \tag{2}$$

where a (soft) Z_2 breaking term m_{12}^2 is introduced. Minimization of the scalar potential determines the vacuum expectation values $\langle\Phi_{1,2}^0\rangle \equiv v_{1,2}/\sqrt{2}$ around which the Higgs doublet fields are expanded as

$$\Phi_{1,2} = \left[\eta_{1,2}^+, \frac{1}{\sqrt{2}}\left(v_{1,2} + \rho_{1,2} + i\eta_{1,2}^0\right)\right]. \tag{3}$$

The model contains the five physical fields in mass eigenstates denoted by $H^\pm, A, H$ and h. Assuming negligible CP violation, $H^\pm$ and A are given by

$$H^\pm, A = s_\beta\, \eta_1^{\pm,0} - c_\beta\, \eta_2^{\pm,0} \tag{4}$$

where the angle β is determined from $t_\beta \equiv \tan\beta = v_2/v_1$, and their orthogonal combinations are the corresponding Goldstone modes $G^{\pm,0}$. The neutral CP-even bosons are diagonalized as

$$h = c_\alpha\, \rho_1 - s_\alpha\, \rho_2, \quad H = s_\alpha\, \rho_1 + c_\alpha\, \rho_2 \tag{5}$$

where $h\,(H)$ denotes the lighter (heavier) state.

The gauge couplings of h and H are given schematically by

$$\mathcal{L}_{\rm gauge} = g_V m_V \big(s_{\beta-\alpha} h + c_{\beta-\alpha} H\big) VV \tag{6}$$

where $V = W^\pm$ or Z. Taking h as the 125 GeV boson of the SM, the SM limit corresponds to $s_{\beta-\alpha} \to 1$. Indeed, LHC finds, $c_{\beta-\alpha} \ll 1$ in all the 2HDMs confirming the SM-like property of the 125 GeV boson [18].

	y_u^A	y_d^A	y_l^A	y_u^H	y_d^H	y_l^H	y_u^h	y_d^h	y_l^h
Type I	$\cot\beta$	$-\cot\beta$	$-\cot\beta$	$\frac{\sin\alpha}{\sin\beta}$	$\frac{\sin\alpha}{\sin\beta}$	$\frac{\sin\alpha}{\sin\beta}$	$\frac{\cos\alpha}{\sin\beta}$	$\frac{\cos\alpha}{\sin\beta}$	$\frac{\cos\alpha}{\sin\beta}$
Type II	$\cot\beta$	$\tan\beta$	$\tan\beta$	$\frac{\sin\alpha}{\sin\beta}$	$\frac{\cos\alpha}{\cos\beta}$	$\frac{\cos\alpha}{\cos\beta}$	$\frac{\cos\alpha}{\sin\beta}$	$-\frac{\sin\alpha}{\cos\beta}$	$-\frac{\sin\alpha}{\cos\beta}$
Type X	$\cot\beta$	$-\cot\beta$	$\tan\beta$	$\frac{\sin\alpha}{\sin\beta}$	$\frac{\sin\alpha}{\sin\beta}$	$\frac{\cos\alpha}{\cos\beta}$	$\frac{\cos\alpha}{\sin\beta}$	$\frac{\cos\alpha}{\sin\beta}$	$-\frac{\sin\alpha}{\cos\beta}$
Type Y	$\cot\beta$	$\tan\beta$	$-\cot\beta$	$\frac{\sin\alpha}{\sin\beta}$	$\frac{\cos\alpha}{\cos\beta}$	$\frac{\sin\alpha}{\sin\beta}$	$\frac{\cos\alpha}{\sin\beta}$	$-\frac{\sin\alpha}{\cos\beta}$	$\frac{\cos\alpha}{\sin\beta}$

TABLE I: The normalized Yukawa couplings for up- and down-type quarks and charged leptons.

Normalizing the Yukawa couplings of the neutral bosons to a fermion f by m_f/v where $v = \sqrt{v_1^2 + v_2^2} = 246$ GeV, we have the following Yukawa terms:

$$\begin{aligned} -\mathcal{L}_{\rm Yukawa}^{\rm 2HDMs} \;=\; & \sum_{f=u,d,l} \frac{m_f}{v} \left(y_f^h h \bar{f} f + y_f^H H \bar{f} f - i y_f^A A \bar{f} \gamma_5 f\right) \\ & + \left[\sqrt{2} V_{ud} H^+ \bar{u} \left(\frac{m_u}{v} y_u^A P_L + \frac{m_d}{v} y_d^A P_R\right) d + \sqrt{2} \frac{m_l}{v} y_l^A H^+ \bar{\nu} P_R l + h.c.\right] \end{aligned} \tag{7}$$

where the normalized Yukawa couplings $y_f^{h,H,A}$ are summarized in Table I for each of these four types of 2HDMs.

Let us now recall that the tau Yukawa coupling $y_\tau \equiv y_l^h$ in Type X (also $y_b \equiv y_d^h$ in Type II) can be expressed as

$$y_\tau = -\frac{s_\alpha}{c_\beta} = s_{\beta-\alpha} - t_\beta c_{\beta-\alpha} \tag{8}$$

which allows us to have the wrong-sign limit $y_\tau \sim -1$ compatible with the LHC data [15] if $c_{\beta-\alpha} \sim 2/t_\beta$ for large $t_\beta \equiv \tan\beta$ favoured by the muon g$-$2. Later we will see that a cancellation in λ_{hAA} can be arranged only for $y_\tau^h < -1$ to suppress the $h \to AA$ decay.

III. THE MUON g$-$2 FROM A LIGHT CP-ODD BOSON

Considering all the updated SM calculations of the muon g$-$2, we obtain

$$a_\mu^{\rm SM} = 116591829\,(57) \times 10^{-11} \tag{9}$$

comparing it with the experimental value $a_\mu^{\rm EXP} = 116592091\,(63) \times 10^{-11}$, one finds a deviation at 3.1σ: $\Delta a_\mu \equiv a_\mu^{\rm EXP} - a_\mu^{\rm SM} = +262\,(85) \times 10^{-11}$. In the 2HDM, the one-loop contributions to a_μ of the neutral and charged bosons are

$$\Delta a_\mu^{\rm 2HDM}(1{\rm loop}) = \frac{G_F\, m_\mu^2}{4\pi^2\sqrt{2}} \sum_j \left(y_\mu^j\right)^2 r_\mu^j\, f_j(r_\mu^j), \tag{10}$$

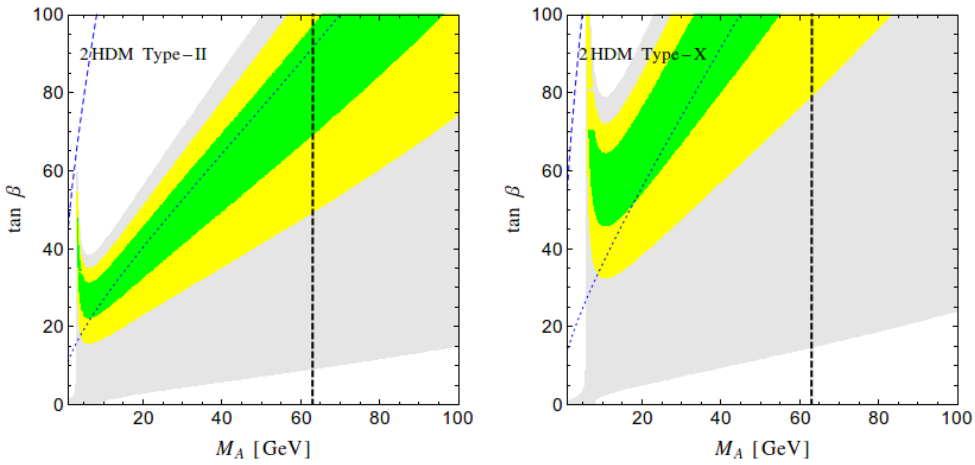

FIG. 2: The 1σ, 2σ and 3σ regions allowed by Δa_μ in the M_A-$\tan\beta$ plane taking the limit of $c_{\beta-\alpha}=0$ and $M_{h(H)}=125$ (200) GeV in type II (left panel) and type X (right panel) 2HDMs. The regions below the dashed (dotted) lines are allowed at 3σ (1.4σ) by Δa_e. The vertical dashed line corresponds to $M_A = M_h/2$.

where $j=\{h,H,A,H^\pm\}$, $r_\mu^j = m_\mu^2/M_j^2$, and

$$f_{h,H}(r) = \int_0^1 dx\, \frac{x^2(2-x)}{1-x+rx^2}, \tag{11}$$

$$f_A(r) = \int_0^1 dx\, \frac{-x^3}{1-x+rx^2}, \tag{12}$$

$$f_{H^\pm}(r) = \int_0^1 dx\, \frac{-x(1-x)}{1-(1-x)r}. \tag{13}$$

These formula show that the one-loop contributions to a_μ are positive for the neutral scalars h and H, and negative for the pseudo-scalar and charged bosons A and $H^\pm$ (for $M_{H^\pm} > m_\mu$). In the limit $r \ll 1$,

$$f_{h,H}(r) = -\ln r - 7/6 + O(r), \tag{14}$$

$$f_A(r) = +\ln r + 11/6 + O(r), \tag{15}$$

$$f_{H^\pm}(r) = -1/6 + O(r), \tag{16}$$

showing that in this limit $f_{H^\pm}(r)$ is suppressed with respect to $f_{h,H,A}(r)$. Now the two-loop Barr-Zee type diagrams with effective $h\gamma\gamma$, $H\gamma\gamma$ or $A\gamma\gamma$ vertices generated by the exchange of heavy fermions gives

$$\Delta a_\mu^{\rm 2HDM}(2{\rm loop}-{\rm BZ}) = \frac{G_F\, m_\mu^2}{4\pi^2\sqrt{2}}\,\frac{\alpha_{\rm em}}{\pi}\sum_{i,f} N_f^c\, Q_f^2\, y_\mu^i\, y_f^i\, r_f^i\, g_i(r_f^i), \tag{17}$$

where $i=\{h,H,A\}$, $r_f^i = m_f^2/M_i^2$, and m_f, Q_f and N_f^c are the mass, electric charge and number of color degrees of freedom of the fermion f in the loop. The functions $g_i(r)$ are

$$g_i(r) = \int_0^1 dx\, \frac{\mathcal{N}_i(x)}{x(1-x)-r}\ln\frac{x(1-x)}{r}, \tag{18}$$

where $\mathcal{N}_{h,H}(x) = 2x(1-x)-1$ and $\mathcal{N}_A(x)=1$.

Note the enhancement factor m_f^2/m_μ^2 of the two-loop formula in Eq. (17) relative to the one-loop contribution in Eq. (10), which can overcome the additional loop suppression factor α/π, and makes the two-loop contributions may become larger than the one-loop ones. Moreover, the signs of the two-loop functions $g_{h,H}$ (negative) and g_A (positive) for the CP-even and CP-odd contributions are opposite to those of the functions $f_{h,H}$ (positive) and f_A (negative) at one-loop. As a result, for small M_A and large $\tan\beta$ in Type II and X, the positive two-loop

pseudoscalar contribution can generate a dominant contribution which can account for the observed Δa_μ discrepancy. The additional 2HDM contribution $\delta a_\mu^{\rm 2HDM} = \delta a_\mu^{\rm 2HDM}(1{\rm loop}) + \delta a_\mu^{\rm 2HDM}(2{\rm loop}-{\rm BZ})$ obtained adding Eqs. (10) and (17) (without the h contributions) is compared with Δa_μ in Fig. 4.

IV. ELECTROWEAK PRECESION DATA

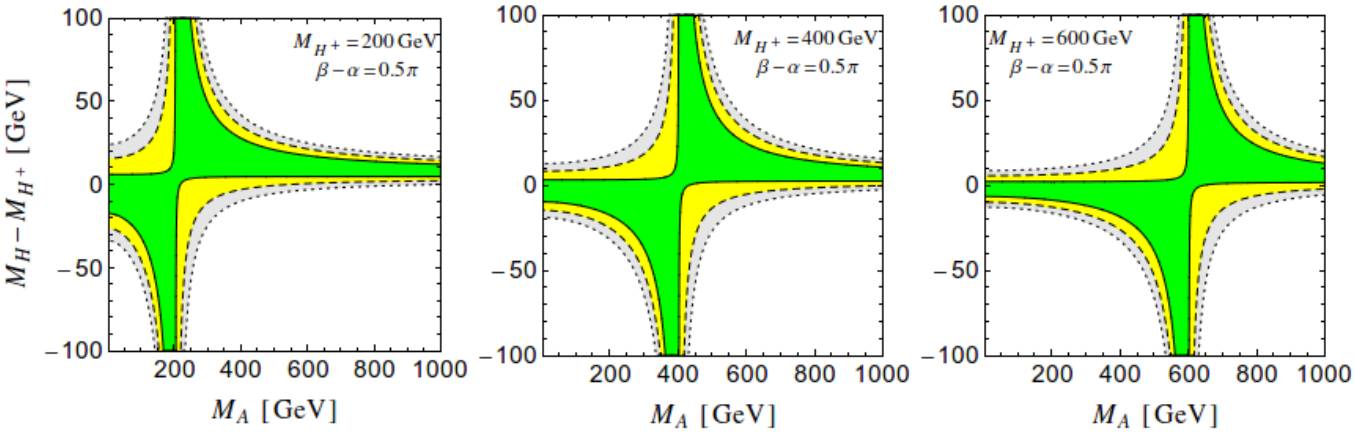

FIG. 3: The parameter space allowed in the M_A vs. $\Delta M_H = M_H - M_{H^\pm}$ plane by the electroweak precision constraints. The green, yellow, gray regions satisfy $\Delta\chi^2_{\rm EW}(M_A, \Delta M) < 2.3, 6.2, 11.8$, corresponding to 68.3, 95.4, and 99.7% confidence intervals, respectively.

Allowing such a light CP-odd boson, there could be a strong limit on the extra boson masses coming from the electroweak precision test. To see this, we compare the theoretical 2HDMs predictions for M_W and $\sin^2\theta_{\rm eff}^{\rm lept}$ with their present experimental values via a combined χ^2 analysis. These quantities can be computed perturbatively by means of the following relations

$$M_W^2 = \frac{M_Z^2}{2}\left[1+\sqrt{1-\frac{4\pi\alpha_{\rm em}}{\sqrt{2}G_F M_Z^2}\frac{1}{1-\Delta r}}\right] \tag{19}$$

$$\sin^2\theta_{\rm eff}^{\rm lept} = k_l(M_Z^2)\sin^2\theta_W\,, \tag{20}$$

where $\sin^2\theta_W = 1 - M_W^2/M_Z^2$, and $k_l(q^2) = 1 + \Delta k_l(q^2)$ is the real part of the vertex form factor $Z \to l\bar{l}$ evaluated at $q^2 = M_Z^2$. We than use the following experimental values:

$$\begin{aligned} M_W^{\rm EXP} &= 80.385 \pm 0.015 \text{ GeV}, \\ \sin^2\theta_{\rm eff}^{\rm lept,EXP} &= 0.23153 \pm 0.00016. \end{aligned} \tag{21}$$

The results of our analysis are displayed in Fig. 3 confirming a custodial symmetry limit [17] of our interest $M_A \ll M_H \sim M_{H^\pm}$, $M_A \sim M_{H^\pm} \ll M_H$, or $M_A \sim M_H \sim M_{H^\pm}$ although the last two cases are disfavoured.

V. THEORETICAL CONSIDERATION OF VACCUM STABILITY AND PERTURBATIVITY

While any value of M_A is allowed by the EW precision tests in the limit of $M_H \sim M_{H^\pm}$, there appear upper bounds on $M_{H^\pm,H}$ by theoretical consideration of vacuum stability, global minimum, and perturbativity expressed

respectively by

$$\lambda_{1,2} > 0, \quad \lambda_3 > -\sqrt{\lambda_1\lambda_2}, \quad |\lambda_5| < \lambda_3 + \lambda_4 + \sqrt{\lambda_1\lambda_2}, \tag{22}$$

$$m_{12}^2(m_{11}^2 - m_{22}^2\sqrt{\lambda_1/\lambda_2})(\tan\beta - (\lambda_1/\lambda_2)^{1/4}) > 0, \tag{23}$$

$$|\lambda_i| \lesssim |\lambda_{\rm max}| = \sqrt{4\pi}, 2\pi, \text{ or } 4\pi. \tag{24}$$

Taking λ_1 as a free parameter, one can have the following expressions for the other couplings in the large t_β limit:

$$\lambda_2 v^2 \approx s_{\beta-\alpha}^2 M_h^2 \tag{25}$$

$$\lambda_3 v^2 \approx 2M_{H^\pm}^2 - (s_{\beta-\alpha}^2 + s_{\beta-\alpha}y_\tau)M_H^2 + s_{\beta-\alpha}y_\tau M_h^2 \tag{26}$$

$$\lambda_4 v^2 \approx -2M_{H^\pm}^2 + s_{\beta-\alpha}^2 M_H^2 + M_A^2 \tag{27}$$

$$\lambda_5 v^2 \approx s_{\beta-\alpha}^2 M_H^2 - M_A^2 \tag{28}$$

where we have used the relation (8) neglecting the terms of $\mathcal{O}(1/t_\beta^2)$.

In the right-sign (RS) limit of the lepton (tau, in particular), $y_\tau s_{\beta-\alpha} \to +1$, one finds a strong upper limit of [6]

$$M_A \ll M_{H^\pm} \sim M_H \lesssim 250\text{GeV} \quad \text{(RS)}. \tag{29}$$

On the other hand, in the wrong-sing (WS) limit, $y_\tau s_{\beta-\alpha} \to -1$, the heavy boson masses up to the perturbativity limit,

$$M_A \ll M_{H^\pm} \sim M_H \lesssim \sqrt{4\pi}v \quad \text{(WS)}. \tag{30}$$

can be obtained.

Let us finally remark that the hAA coupling is generically order one and thus can leads to a sizable non-standard decay of $h \to AA$ or $AA^*(\tau\tau)$ if allowed kinematically. Then, one needs to have $|\lambda_{hAA}/v| \ll 1$ to avoid an exotic decay of the SM boson. Noting that $\lambda_{hAA}/v \approx s_{\beta-\alpha}[\lambda_3 + \lambda_4 - \lambda_5]$, one gets

$$\lambda_{hAA}v/s_{\beta-\alpha} \approx -(1 + s_{\beta-\alpha}y_\tau)M_H^2 + s_{\beta-\alpha}y_\tau M_h^2 + 2M_A^2 \tag{31}$$

where we have put $s_{\beta-\alpha}^2 = 1$. In the RS or SM limit, the condition $\lambda_{hAA} \approx 0$ can be met for a rather light H with $M_H^2 \approx \frac{1}{2}M_h^2 + M_A^2$ which is disfavoured in the explanation of the muon g–2. On the other hand, one can arrange a cancellation for $\lambda_{hAA} \approx 0$ in the wrong-sign limit for arbitrary value of M_H if the tau Yukawa coupling satisfies

$$y_\tau s_{\beta-\alpha} \approx -\frac{M_H^2 - 2M_A^2}{M_H^2 - M_h^2} < -1. \tag{32}$$

VI. LEPTON UNIVERSALITY TESTS

In the limit of large $\tan\beta$, the charged boson can generate significant corrections to τ decays at the tree level and furthermore the extra Higg boson contribution to one-loop corrections can also be significant [19]. The recent study [8] showed that a stringent bound on the charged boson contributions can be obtained from the lepton universality condition obtained by the HFAG collaboration [14]. Given the precision at the level of 0.1 %, the lepton universality data put the strongest bound on the type X 2HDM parameter space in favor of the muon g–2. Thus, let us now make a proper analysis of the HFAG data.

From the measurements of the pure leptonic processes, $\tau \to \mu\nu\nu$, $\tau \to e\nu\nu$ and $\mu \to e\nu\nu$, HFAG obtained the constraints on the three coupling ratios, $(g_\tau/g_\mu) = \sqrt{\Gamma(\tau \to e\nu\nu)/\Gamma(\mu \to e\nu\nu)}$, etc. Defining $\delta_{ll'} \equiv (g_l/g_{l'}) - 1$, let us rewrite the data from the leptonic processes:

$$\delta_{\tau\mu}^l = 0.0011 \pm 0.0015, \quad \delta_{\tau e}^l = 0.0029 \pm 0.0015, \quad \delta_{\mu e}^l = 0.0018 \pm 0.0014 \tag{33}$$

In addition, combing the semi-hadronic processes $\pi/K \to \mu\nu$, HFAG also provided the averaged constraint on (g_τ/g_μ) which is translated into

$$\delta_{\tau\mu}^{l+\pi+K} = 0.0001 \pm 0.0014. \tag{34}$$

It is important to notice that only two ratios out of the three leptonic measurements are independent and thus the three data (33) are strongly correlated. For a consistent treatment of the data, one combination out of the three has to be projected out. One can indeed check that the direction $\delta^l_{\tau\mu} - \delta^l_{\tau e} + \delta^l_{\mu e}$ has the zero best-fit value and the zero eigenvalue of the covariance matrix, and thus corresponds to the unphysical direction. Furthermore, two orthogonal directions $\delta^l_{\tau\mu} + \delta^l_{\tau e}$ and $-\delta^l_{\tau\mu} + \delta^l_{\tau e} + 2\delta^l_{\mu e}$ are found to be uncorrelated in a good approximation. As a result, the 2HDM contribution to $\delta_{ll'}$ are calculated to be

$$\delta^l_{\tau\mu} = \delta_{loop}, \quad \delta^l_{\tau e} = \delta_{tree} + \delta_{loop}, \quad \delta^l_{\mu e} = \delta_{tree}, \quad \delta^{l+\pi+K}_{\tau\mu} = \delta_{loop}. \tag{35}$$

Here δ_{tree} and δ_{loop} are given by [19]:

$$\begin{aligned} \delta_{tree} &= \frac{m_\tau^2 m_\mu^2}{8 m_{H^\pm}^4} \tan^4\beta - \frac{m_\mu^2}{m_{H^\pm}^2} t_\beta^2 \frac{g(m_\mu^2/m_\tau^2)}{f(m_\mu^2/m_\tau^2)}, \\ \delta_{loop} &= \frac{G_F m_\tau^2}{8\sqrt{2}\pi^2} t_\beta^2 \left[1 + \frac{1}{4}\left(H(x_A) + s^2_{\beta-\alpha} H(x_H) + c^2_{\beta-\alpha} H(x_h)\right)\right]. \end{aligned} \tag{36}$$

where $f(x) \equiv 1 - 8x + 8x^3 - x^4 - 12x^2\ln(x)$, $g(x) \equiv 1 + 9x - 9x^2 - x^3 + 6x(1+x)\ln(x)$, $H(x) \equiv \ln(x)(1+x)/(1-x)$, and $x_\phi = m_\phi^2/m_{H^\pm}^2$. From Eqs. (33), (34) and (35), one obtains the following three independent bounds:

$$\begin{aligned} \frac{1}{\sqrt{2}}\delta_{tree} + \sqrt{2}\delta_{loop} &= 0.0028 \pm 0.0019, \\ \sqrt{\frac{3}{2}}\delta_{tree} &= 0.0022 \pm 0.0017, \\ \delta_{loop} &= 0.0001 \pm 0.0014. \end{aligned} \tag{37}$$

We will use these constraints to put a strong limit on the $(g-2)_\mu$ favoured region in the M_A–$\tan\beta$ plane in the next section. Let us recall that the $Z \to \tau\tau$ data, although less strong than the HFAG data, provides an independent bound [8] which further cuts out some corner of parameter space.

VII. PINNING DOWN THE WHOLE 2HDM-X PARAMETER SPACE

It is an interesting task to narrow down the allowed region of the type X 2HDM parameter space collecting all the relevant experimental data including those outlined in Section I and the 125 GeV boson data from LHC, in particular. The scan ranges of all the 2HDM-X input parameters are listed in Table II. For our scan, we adopt the convention $-\pi/2 < \alpha - \beta < \pi/2$ and $0 < \beta < \pi/2$, and use the parameter λ_1 as an input parameter instead of m_{12}^2.

2HDM parameter	Range
Scalar boson mass (GeV)	$125 < m_H < 400$
Pseudoscalar boson mass (GeV)	$10 < m_A < 400$
Charged boson mass (GeV)	$94 < m_{H^\pm} < 400$
$c_{\beta-\alpha}$	$0.0 < c_{\beta-\alpha} < 0.1$
$\tan\beta$	$10 < \tan\beta < 150$
λ_1	$0.0 < \lambda_1 < 4\pi$

TABLE II: The scan ranges of the 2HDM-X input parameters.

Fig. 4 shows the allowed region in the m_A-$\tan\beta$ plane from the profile-likelihood study taking all the other 2HDM-X parameters as nuisance parameters. To see the impact of the lepton universality data by HFAG, we overlay the contour lines of the lepton universality likelihood at the 99%, 95% and 90% confidence level based on the constraints (37). The allowed region opened up for $\tan\beta > 140$ needs a comment. Note that the δ_{loop} is always negative while δ_{tree} becomes positive for larger $\tan\beta/m_{H^\pm}$. Thus, there appears a fine-tuned region around $\tan\beta/m_{H^\pm} \sim 1$ GeV^{-1}

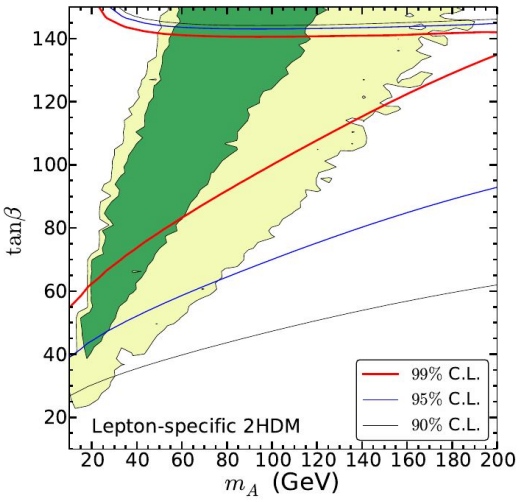

FIG. 4: The 68% and 95% allowed regions by Δa_μ and other experimental constraints in the m_A-tan β plane. The contours of the lepton universality likelihood in the 99%, 95% and 90% confidence level are overlayed.

where the positive δ_{tree} and the negative δ_{loop} cancel each other to give a good fit. However, such regions are excluded by the $Z \to \tau\tau$ data [8] and thus we are left with the tightly limited region of $M_A \approx 10 - 80$ GeV and $\tan\beta \approx 25 - 60$ at the 95% confidence level.

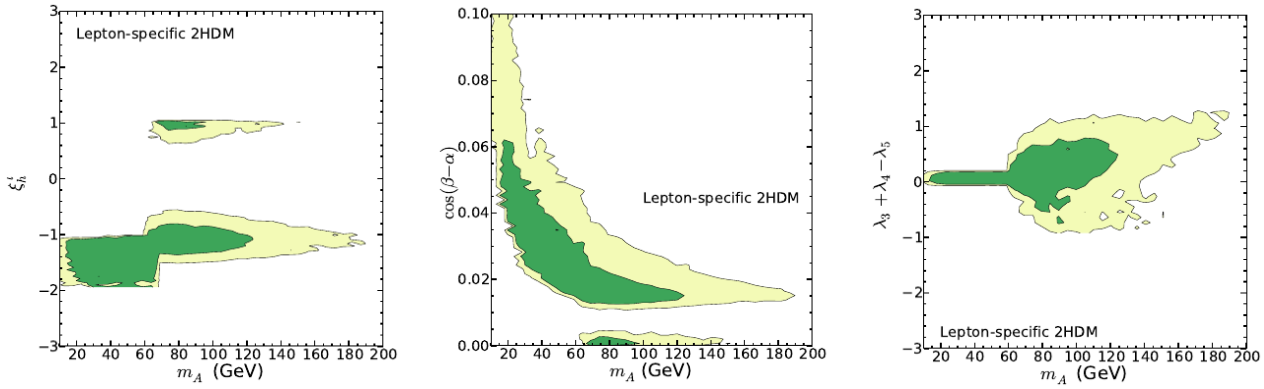

FIG. 5: The 68% and 95% allowed regions in the m_A–ξ_h^l ($y_\tau \equiv \xi_h^l$) (left) and m_A–$c_{\beta-\alpha}$ (middle), and m_A–λ_{hAA} ($\lambda_{hAA} \approx \lambda_3 + \lambda_4 - \lambda_5$) (right) plane.

The region allowed in Fig. 4 can be either in the right-sign ($y_\tau \equiv \xi_h^l > 0$) or wrong-sign ($y_\tau \equiv \xi_h^l < 0$) domain as shown in the left and middle panels of Fig. 5. One can see that the rigt-sign limit is tightly constrained to a small region of $m_A \approx 60 - 80$ GeV while the wrong-sign limit is favoured in a wider range of parameter space. The right panel shows the sizes of the coupling λ_{hAA} restricted by the LHC data on the exotic decay of the 125 GeV boson, putting a generous bound of $\mathrm{Br}(h \to AA^{(*)}) < 40\%$. As explained before, the suppressed value of λ_{hAA} for $m_A \lesssim m_h/2$ is shown to appear only in the wrong-sign domain.

Given the possible existence of a light CP-odd boson explaining the muon g–2 in the type X 2HDM, it would be important to look for its trails at the LHC. Fig. 6 shows the allowed mass ranges of all the extra bosons. Region A following the pattern of $m_A \lesssim m_H \approx m_{H^\pm}$ is favoured while Region B with $m_A \approx m_{H^\pm} \ll m_H$ is already excluded as discussed before.

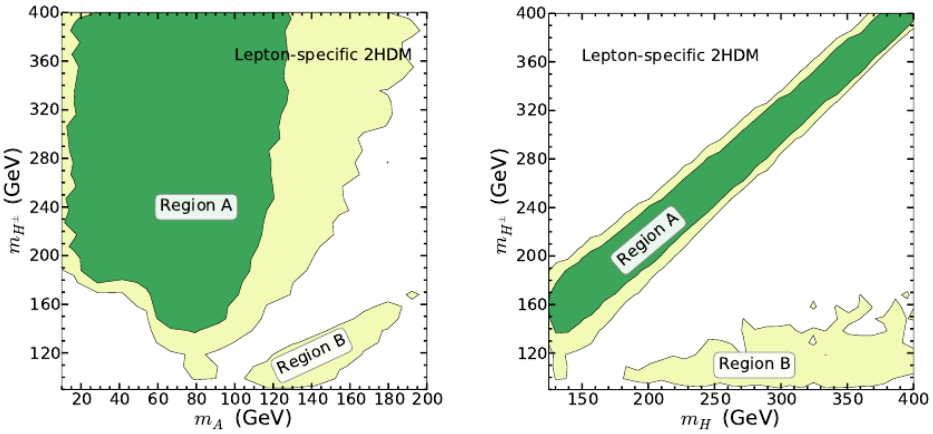

FIG. 6: Distribution of the extra boson masses allowed at the 68% and 95% confidence levels.

VIII. TAU-RICH SIGANTURES AT THE LHC

The bulk parameter space with $m_A \ll m_H \sim m_{H^\pm}$ is a clear prediction of the type X 2HDM as the origin of the muon g–2 anomaly. Since the extra bosons are mainly from the "leptonic" Higgs doublet with large $\tan\beta$, all the three members are expected to dominantly decay into the $\tau-$flavor, leading to $\tau-$rich signatures at the LHC via the following production and ensuing cascade decay chains:

$$\begin{aligned} pp \to & W^{\pm *} \to H^\pm A \to (\tau^\pm \nu)(\tau^+\tau^-), \\ pp \to & Z^*/\gamma^* \to HA \to (\tau^+\tau^-)(\tau^+\tau^-), \\ pp \to & W^{\pm *} \to H^\pm H \to (\tau^\pm \nu)(\tau^+\tau^-), \\ pp \to & Z^*/\gamma^* \to H^+H^- \to (\tau^+\nu)(\tau^-\bar{\nu}). \end{aligned} \tag{38}$$

To probe Region A, we select six benchmark points with different combinations of m_A and m_H presented in Table III. For each point, we take a simple parametrization of $\tan\beta = 1.25(m_A/\text{GeV}) + 25$ and $m_{H^\pm} = m_H + 15\text{GeV}$. Note that we included the points with $m_A > 80$ GeV for the sake of the LHC study although they are forbidden by the lepton universality tests. In Table III, we show the production cross-section, the selection cuts and the significance for each benchmark expected for the integrated luminosity of 25/fb at the 14 TeV LHC.

	point A	point B	point C	point D	point E	point F
m_A [GeV]	20	40	100	40	100	180
m_H [GeV]	200	200	200	260	260	260
total σ_{gen} [fb]	270.980	241.830	153.580	100.430	71.271	44.163
$n_\ell \geq 3$	6.606	16.681	21.713	7.110	11.962	8.822
$n_\tau \geq 3$	0.894	2.602	4.386	0.888	2.346	1.971
$\not{E}_T > 100$ GeV	0.201	0.547	1.179	0.209	0.765	0.926
$n_b = n_j = 0$	0.098	0.314	0.857	0.121	0.479	0.631
S/B	0.1	0.5	1.2	0.2	0.7	0.9
$S/\sqrt{B}_{25\text{fb}^{-1}}$	0.6	1.9	5.2	0.7	2.9	3.8

TABLE III: The number of events after applying successive cuts for 14 TeV LHC.

In Fig. 7, we present the exclusion region coming mainly from the chargino-neutralino search at the LHC8, and the expected discovery reaches at LHC14 with the integrated luminosity of 25/fb. A heavy CP-even boson with $m_H > 200$ GeV and a light CP-odd boson with $m_A < 50$ GeV are still allowed, and the LHC14 can explore some

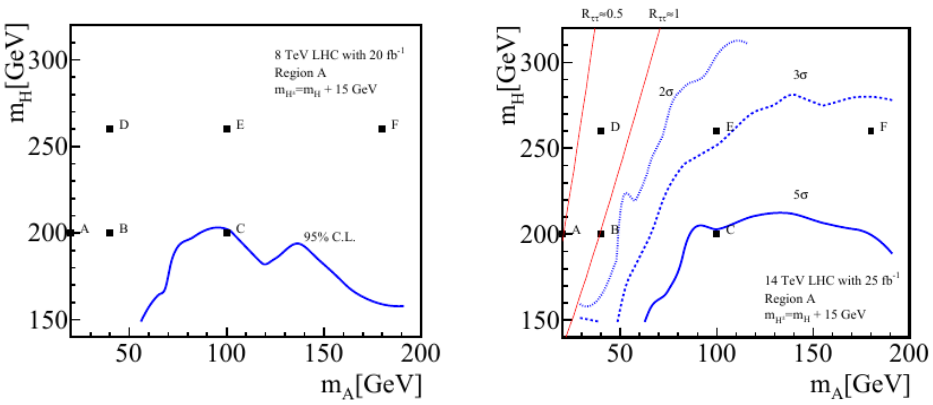

FIG. 7: The 95% exclusion contour from LHC8 (left) and the 2σ, 3σ and 5σ discovery reach countours at LHC14 (right) in the m_A–m_H plane.

of the regions. The sensitivities are weaker for larger m_H just because of smaller cross sections, and for smaller m_A because τs from lighter A become softer and thus the acceptance quickly decreases. Moreover, the $H/H^\pm \to AZ/W^\pm$ decay modes also start open to decrease the number of hard τs from direct $H/H^\pm$ decays. In such a region, a light A from heavy H^+/H decay will be boosted, resulting in a collimated $\tau-$pair which becomes difficult to be tagged as two separated τ-jets. It is one of the reasons to have less acceptance for this parameter region. We can estimate the separation $R_{\tau\tau}$ of the τ leptons from A decay:

$$R_{\tau\tau} \sim \frac{2m}{p_T} \sim \frac{4m_A}{m_{H^\pm/H}\sqrt{1-2\frac{m_A^2+m_{W/Z}^2}{m_{H^\pm/H}^2}+\frac{(m_A^2-m_{W/Z}^2)^2}{m_{H^\pm/H}^4}}}. \tag{39}$$

Since the jets are usually defined with $R = 0.5$, the $\tau-$pair starts overlapping. We indicated the region with the overlapping τ problem in red lines in the right panel of Fig. 7. Further studies on how to capture the kinematic features of the boosted $A \to \tau^+\tau^-$ are required to probe such a small m_A region.

IX. SUMMARY

The type X 2HDM is still a viable option for the explanation of the muon g–2 in the parameter region with large $\tan\beta$ and a light CP-odd boson A. Being "hadrophobic and leptophilic" in the large $\tan\beta$ limit, it can be easily free from all the hadron-related constraints, particularly, coming from the decay $B_s \to \mu\mu$ which puts only a mild bound of $m_A \gtrsim 10$ GeV. However, such a region is tightly limited by the lepton universality tests from the HFAG and $Z \to \tau\tau$ data. Combining all the current bounds, we find allowed at the 95% confidence level a limited region of $\tan\beta \approx 15 - 60$ and $m_A \approx 10 - 80$ GeV with $m_H \approx m_{H^\pm} \gg m_A$.

It will be an interesting task to search for such a light CP-odd boson A and the extra heavy bosons $H, H^\pm$ in the next run of the LHC mainly through $pp \to AH, AH^\pm$ followed by the decays $H^\pm \to \tau^\pm\nu$ and $A, H \to \tau^+\tau^-$ which requires further studies to improve the (boosted) tau identification.

[1] H. N. Brown *et al.* [Muon g-2 Collaboration], Phys. Rev. Lett. **86** (2001) 2227 [hep-ex/0102017]. G. W. Bennett *et al.* [Muon g-2 Collaboration], Phys. Rev. D **73** (2006) 072003 [hep-ex/0602035].

[2] A. Dedes and H. E. Haber, JHEP **0105** (2001) 006 [hep-ph/0102297]. K. m. Cheung, C. H. Chou and O. C. W. Kong, Phys. Rev. D **64** (2001) 111301 [hep-ph/0103183]. M. Krawczyk, hep-ph/0103223. F. Larios, G. Tavares-Velasco and C. P. Yuan, Phys. Rev. D **64** (2001) 055004 [hep-ph/0103292].

[3] M. Krawczyk, Acta Phys. Polon. B **33** (2002) 2621 [hep-ph/0208076].
[4] K. Cheung and O. C. W. Kong, Phys. Rev. D **68** (2003) 053003 [hep-ph/0302111].
[5] J. Cao, P. Wan, L. Wu and J. M. Yang, Phys. Rev. D **80** (2009) 071701 [arXiv:0909.5148 [hep-ph]].
[6] A. Broggio, E. J. Chun, M. Passera, K. M. Patel and S. K. Vempati, JHEP **1411** (2014) 058 [arXiv:1409.3199 [hep-ph]].
[7] L. Wang and X. F. Han, JHEP **1505** (2015) 039 [arXiv:1412.4874 [hep-ph]].
[8] T. Abe, R. Sato and K. Yagyu, JHEP **1507** (2015) 064 [arXiv:1504.07059 [hep-ph]].
[9] E. J. Chun, Z. Kang, M. Takeuchi and Y.-L. Sming Tsai, to apear in JHEP [arXiv:1507.08067 [hep-ph]].
[10] S. M. Barr and A. Zee, Phys. Rev. Lett. 65 (1990) 21 [Erratum-ibid. 65 (1990) 2920]. V. Ilisie, arXiv:1502.04199 [hep-ph].
[11] H. E. Logan and U. Nierste, Nucl. Phys. B **586** (2000) 39 [hep-ph/0004139].
[12] CMS and LHCb Collaboration, CMS-PAS-BPH-13-007.
[13] K. Schmidt-Hoberg, F. Staub and M. W. Winkler, Phys. Lett. B **727** (2013) 506 [arXiv:1310.6752 [hep-ph]].
[14] HFAG Collaboration, arXiv:1412.7515 [hep-ph].
[15] P. M. Ferreira, J. F. Gunion, H. E. Haber and R. Santos, Phys. Rev. D **89** (2014) 11, 115003 [arXiv:1403.4736 [hep-ph]]. P. M. Ferreira, R. Guedes, M. O. P. Sampaio and R. San tos, JHEP **1412** (2014) 067 [arXiv:1409.6723 [hep-ph]].
[16] J. F. Gunion and H. E. Haber, Phys. Rev. D **67** (2003) 075019 [hep-ph/0207010]. G. C. Branco, P. M. Ferreira, L. Lavoura, M. N. Rebelo, M. Sher and J. P. Silva, Phys. Rept. **516** (2012) 1 [arXiv:1106.0034 [hep-ph]].
[17] J.-M. Gerard and M. Herquet, Phys. Rev. Lett. **98** (2007) 251802 [hep-ph/0703051 [HEP-PH]].
[18] ATLAS Collaboration, arXiv:1509.00672; D. Chowdhury and O. Eberhardt, arXiv:1503.08216 [hep-ph].
[19] M. Krawczyk and D. Temes, arXiv:hep-ph/0410348.